



DYNAMIC STIFFNESS FORMULATION AND FREE VIBRATION ANALYSIS OF CENTRIFUGALLY STIFFENED TIMOSHENKO BEAMS

J. R. BANERJEE

Department of Mechanical Engineering and Aeronautics, City University, Northampton Square, London EC1V 0HB, England. E-mail: j.r.banerjee@city.ac.uk

(Received 24 October 2000, and in final form 6 March 2001)

The dynamic stiffness matrix of a centrifugally stiffened Timoshenko beam has been developed and used to carry out a free vibration analysis. The governing differential equations of motion of the beam in free vibration are derived using Hamilton's principle and include the effect of an arbitrary hub radius. For harmonic oscillation the derivation leads to two different (but of similar form) fourth-order ordinary differential equations with variable coefficients that govern the amplitudes of bending displacement and bending rotation respectively. An outboard force at the end of the beam is taken into account which makes possible the free vibration analysis of rotating non-uniform or tapered Timoshenko beams. Using the Frobenius method of series solution and imposing boundary conditions, the dynamic stiffness matrix, which relates amplitudes of harmonically varying forces with the amplitudes of harmonically varying displacements at the ends of the element, is formulated. Applying the Wittrick–Williams algorithm to the resulting dynamic stiffness matrix the natural frequencies of a few carefully chosen illustrative examples are obtained. The results are compared with those available in the literature. © 2001 Academic Press

1. INTRODUCTION

The free vibration analysis of a centrifugally stiffened Bernoulli–Euler beam has been carried out by a number of investigators using different methods [1–6]. Recently, a contribution has been made to this literature by the present author who developed for the first time a dynamic stiffness matrix to study the free vibration characteristics of rotating uniform and non-uniform Bernoulli–Euler beams [7]. The superiority of the dynamic stiffness method over finite element and other approximate methods in predicting the natural frequencies and mode shapes of structures or structural elements accurately is well known [8–10]. It is also commonly accepted that the Timoshenko beam theory, which accounts for the effects of shear deformation and rotatory inertia, is more accurate than the Bernoulli–Euler beam theory, particularly when the cross-sectional dimensions of the beam are relatively large, and when higher natural frequencies are required. Thus, the solution of the free vibration problems of rotating Timoshenko beams using the dynamic stiffness method is a natural extension of the author's recent work [7]. There are of course, a number of published papers on the subject of rotating Timoshenko beams [11–16] and on various similar aspects of non-rotating structures [17–22] using other methods. This new development of dynamic stiffness theory is of considerable complexity, requiring substantial analytical and computational efforts. The main focus of this research is to investigate the

free vibration characteristics of rotating Timoshenko beams by extending the elegant power of the dynamic stiffness method.

This research is partly motivated by two recent papers [14, 15] on the subject in which an inaccurate differential equation has unfortunately been used when solving the free vibration problem of rotating Timoshenko beams. In particular, a significant term related to the rotational speed was omitted in these papers by their authors while formulating the governing differential equations of motion for the problem and thus devaluing the theory. As a consequence the numerical results reported [14, 15] are not sufficiently accurate (particularly for higher rotational speeds). This, of course, contradicts the claim made by the authors of reference [15] that their theory provides a benchmark solution to the problem (see the last line of their conclusions). In the analysis presented below the inaccuracies of references [14, 15] are corrected and the problem is addressed in a judicious manner using a new approach based on the dynamic stiffness solution to the problem. The results from the present theory are contrasted with those reported in references [14, 15].

The investigation is carried out in the following steps. First, the governing differential equations of motion of a rotating Timoshenko beam undergoing free natural vibration are derived using Hamilton's principle. Assuming harmonic oscillation the equations are then solved using the Frobenius method of series solution. Next, the boundary conditions for bending displacements, bending rotation, shear force and bending moment are imposed and the arbitrary constants are eliminated from the general solution. This essentially recasts the ensuing equations in the form of a dynamic stiffness matrix of a rotating Timoshenko beam element, relating amplitudes of harmonically varying forces with amplitudes of harmonically varying displacements at its ends. Finally, the resulting dynamic stiffness matrix is applied using the Wittrick-Williams algorithm [23] to obtain natural frequencies of some carefully chosen examples. The results are compared with published results and some conclusions are drawn.

2. THEORY

Figure 1(a) shows in a rectangular Cartesian co-ordinate system, the notation used for a rotating Timoshenko beam which has four uniform parts AB, BC, CD and DE, respectively, with each having uniform properties so that the assembly forms a stepped beam. The hub radius and the rotational speed are taken to be r_H and Ω , respectively, as shown. A typical element BC (shown by the solid line in Figure 1(a)) which forms a part of the whole assembly is shown separately in Figure 1(b). This element will be considered here in the dynamic stiffness analysis. It is essential that the dynamic stiffness matrix to be derived can be assembled for a number of such elements to form the dynamic stiffness matrix of the complete structure. This enables free vibration analysis of rotating tapered or non-uniform Timoshenko beams. The origin of the element (see Figure 1(b)) is taken at the left-hand end and is at a distance r_i from the axis of rotation. The Y -axis is considered to be coincident with the centroidal axis of the beam whereas the Z -axis is parallel, but not coincidental with the axis of rotation of the beam. (Due to the choice of right-handed co-ordinate system, the X -axis is perpendicular and away from the plane of the paper.) The total length of the stepped beam in Figure 1(a) is L_T whereas the length of the typical element BC in Figure 1(b) is L . An outboard force F at the right-hand end of the element BC that may arise as a result of the adjacent elements CD and DE is taken into account when developing the theory. Clearly, for the element DE, this force is zero.

Attention is here confined to the derivation of the dynamic stiffness matrix corresponding to the out-of-plane vibration of the beam in the YZ -plane only. The corresponding dynamic

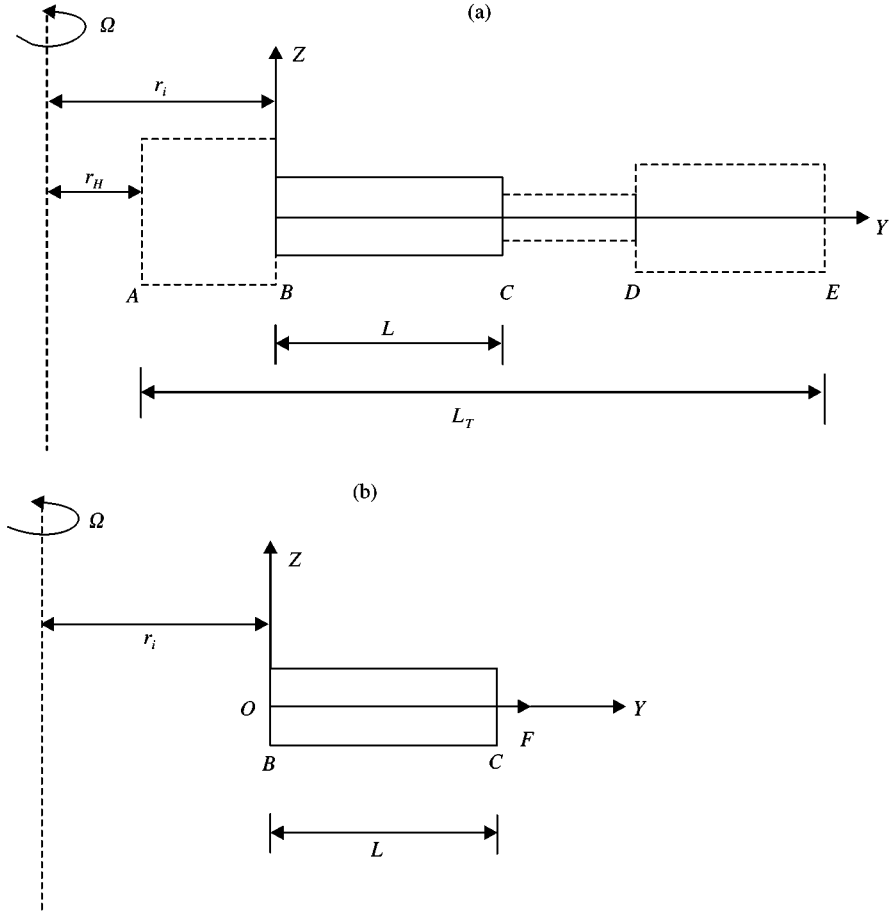


Figure 1. (a) Co-ordinate system and notation for a rotating Timoshenko beam formed by four uniform elements so as to form a stepped beam of length L_T ; (b) Co-ordinate system and notation for a rotating Timoshenko beam element of length L .

stiffness matrix related to the in-plane vibration in the XY -plane of the beam can be derived by following the same procedure and by suitable substitution of beam parameters [4, 7].

The two governing partial differential equations of motion for free vibration in the YZ -plane of the Timoshenko beam BC are derived using Hamilton's principle (see Appendix A for details). They are

$$(Tw') - \rho A \ddot{w} + kAG(w'' - \theta') = 0, \quad EI\theta'' + kAG(w' - \theta) - \rho I \ddot{\theta} + \rho I \Omega^2 \theta = 0, \quad (1, 2)$$

where T , the centrifugal tension at a distance y from the origin, is given by [7]

$$T(y) = \Omega^2 \rho A [r_i L + \frac{1}{2} L^2 - r_i y - \frac{1}{2} y^2] + F, \quad (3)$$

EI and kAG are, respectively, the bending and shear rigidity, ρ is the density of the material, A is the area of cross-section (so that ρA is the mass per unit length), I is the second moment of area of the beam cross-section about the X -axis. A prime and an over dot denote differentiation with respect to distance y and time t respectively.

Equations (1) and (2) define completely the free vibration characteristics of a uniform rotating Timoshenko beam. Note that the term $\rho I \Omega^2 \theta$ in equation (2) which can be

significant for higher rotational speed Ω , is omitted by the authors of references [14, 15]. The physical origin of this term lies in the fact that the centrifugal force on elements symmetrically placed with respect to the mid-plane of the beam cross-section have different radii from the axis of rotation when undergoing bending deformation, and so have different centrifugal forces. This generates a moment which is $\rho I \Omega^2 \theta$. (The corresponding net centrifugal force is independent of section rotation.) For harmonic oscillation the term $\rho I \Omega^2 \theta$ indicates an increase in rotatory inertia of the element, see equation (2).

Assuming simple harmonic oscillation, w and θ can be written as

$$w(y, t) = W(y) e^{i\omega t}, \quad \theta(y, t) = \Theta(y) e^{i\omega t}. \quad (4)$$

Substituting equation (4) into equations (1) and (2) and introducing the non-dimensional parameter

$$\xi = y/L \quad (5)$$

it can be shown, after considerable algebraic manipulation, that equations (1) and (2) with the help of equation (4) can be expressed as two different, but similar, fourth order ordinary differential equations with variable coefficients as follows. (Note that for a centrifugally stiffened Bernoulli–Euler beam the formulation leads to only one differential equation which applies to both the bending displacement and the bending rotation [7].)

$$\begin{aligned} (C_1 + C_2 \xi + C_3 \xi^2) \frac{d^4 W}{d\xi^4} + (C_4 + C_5 \xi) \frac{d^3 W}{d\xi^3} + (C_6 + C_7 \xi + C_8 \xi^2) \frac{d^2 W}{d\xi^2} \\ + (C_9 + C_{10} \xi) \frac{dW}{d\xi} + C_{11} W = 0, \end{aligned} \quad (6)$$

$$\begin{aligned} (C_1^* + C_2^* \xi + C_3^* \xi^2) \frac{d^4 \Theta}{d\xi^4} + (C_4^* + C_5^* \xi) \frac{d^3 \Theta}{d\xi^3} + (C_6^* + C_7^* \xi + C_8^* \xi^2) \frac{d^2 \Theta}{d\xi^2} \\ + (C_9^* + C_{10}^* \xi) \frac{d\Theta}{d\xi} + C_{11}^* \Theta = 0, \end{aligned} \quad (7)$$

where

$$C_1 = 1 + \eta^2 s^2 (\alpha + \frac{1}{2}) + p^2 s^2, \quad C_1^* = C_1; \quad C_2 = -\eta^2 s^2 \alpha, \quad C_2^* = C_2, \quad (8, 9)$$

$$C_3 = -\frac{1}{2} \eta^2 s^2, \quad C_3^* = C_3; \quad C_4 = -3\eta^2 s^2 \alpha, \quad C_4^* = 2C_2; \quad C_5 = -3\eta^2 s^2, \quad C_5^* = 4C_3, \quad (10-12)$$

$$C_6 = \eta^2 \zeta (\alpha + \frac{1}{2}) + (r^2 + s^2)(\mu^2 + \eta^2) + p^2 \zeta - 4\eta^2 s^2, \quad C_6^* = C_6 - 4C_3, \quad (13)$$

$$C_7 = -\eta^2 \zeta \alpha, \quad C_7^* = C_7; \quad C_8 = -\frac{1}{2} \eta^2 \zeta, \quad C_8^* = C_8; \quad C_9 = C_7, \quad C_9^* = 2C_7. \quad (14-16)$$

$$C_{10} = 2C_8, \quad C_{10}^* = 4C_8; \quad C_{11} = \mu^2 \zeta, \quad C_{11}^* = C_{11} + 2C_8 \quad (17, 18)$$

with

$$r^2 = \frac{I}{AL^2}, \quad s^2 = \frac{EI}{kAGL^2}, \quad p^2 = \frac{FL^2}{EI}, \quad \xi = \frac{y}{L}, \quad \alpha = \frac{r_H}{L}, \quad \eta^2 = \frac{\rho A}{EI} L^4 \Omega^2, \quad \mu^2 = \frac{\rho AL^4 \omega^2}{EI} \quad (19)$$

and

$$\zeta = r^2 s^2 (\mu^2 + \eta^2) - 1. \quad (20)$$

The differential equations (6) and (7) are of the same form and are amenable to power series solution in terms of the independent variable ξ . Note that for a non-rotating Timoshenko beam ($\eta = 0$) the two differential equations become identical which accords with the formulation given by Howson and Williams [24]. The solutions of the differential equations (6) and (7) will be of the same form provided the constants C_1 – C_{11} and C_1^* – C_{11}^* are interpreted correctly. Using the method of Frobenius, the solution is sought in the form of the following series [4, 7, 15]:

$$Y(c, \xi) = \sum_{n=0}^{\infty} a_{n+1}(c) \xi^{c+n}, \quad (21)$$

where a_{n+1} are the coefficients and c is an undetermined exponent. Substituting equation (21) into equation (6) or (7), one obtains the following indicial equation [4, 7, 15]:

$$c(c-1)(c-2)(c-3) = 0, \quad (22)$$

and the following recurrence relationship:

$$\begin{aligned} a_{n+5}(c) = & -a_{n+4}(c) \frac{C_2(c+n) + C_4}{C_1(c+n+4)} - a_{n+3}(c) \frac{C_3(c+n)(c+n-1) + C_5(c+n) + C_6}{C_1(c+n+4)(c+n+3)} \\ & - a_{n+2}(c) \frac{C_7(c+n) + C_9}{C_1(c+n+4)(c+n+3)(c+n+2)} \\ & - a_{n+1}(c) \frac{C_8(c+n)(c+n-1) + C_{10}(c+n) + C_{11}}{C_1(c+n+4)(c+n+3)(c+n+2)(c+n+1)}, \quad n \geq 0 \end{aligned} \quad (23)$$

where the first four coefficients can be defined with the help of equations (6) (or (7)) and (21) as follows. (Note that this formulation is similar to, but different from that of reference [15] because in equation (21), ξ^{c+n} , instead of ξ^n , has been used.)

$$a_1(0) = 1, \quad a_2(0) = 0, \quad a_3(0) = 0, \quad a_4(0) = 0. \quad (24)$$

$$a_1(1) = 1, \quad a_2(1) = 0, \quad a_3(1) = 0, \quad a_4(1) = -C_9/(24C_1), \quad (25)$$

$$a_1(2) = 1, \quad a_2(2) = 0, \quad a_3(2) = -C_6/(12C_1), \quad a_4(2) = \{C_6(C_2 + C_4) - C_1(C_7 + C_9)\}/(60C_1^2), \quad (26)$$

$$\begin{aligned} a_1(3) = 1, \quad a_2(3) = & -C_4/(4C_1), \quad a_3(3) = \{C_4(C_2 + C_4) - C_1(C_5 + C_6)\}/(20C_1^2), \\ a_4(3) = & -[(2C_2 + C_4)\{C_4(C_2 + C_4) - C_1(C_5 + C_6)\} - C_1C_4(2C_3 + 2C_5 + C_6) \\ & + C_1^2(2C_7 + C_9)]/(120C_1^3). \end{aligned} \quad (27)$$

Equations (23)–(27) apply for the solution of W , but they can also be applied for the solution of Θ provided that C_1 – C_{11} are replaced by C_1^* – C_{11}^* . (In order to avoid confusion on asterisk has been introduced to designate the terms as a_{n+1}^* to be used for the solutions of Θ .)

The roots of the indicial equation (22) are $c = 0, 1, 2, 3$ so that the solutions for W and Θ of each of equations (6) and (7) can be expressed as linear combinations of four independent solutions as

$$W(\xi) = A_1 Y(0, \xi) + A_2 Y(1, \xi) + A_3 Y(2, \xi) + A_4 Y(3, \xi), \quad (28)$$

$$\Theta(\xi) = B_1 \Psi(0, \xi) + B_2 \Psi(1, \xi) + B_3 \Psi(2, \xi) + B_4 \Psi(3, \xi), \quad (29)$$

where A_1 - A_4 and B_1 - B_4 are two different sets of constants and

$$Y(0, \zeta) = 1 + a_5(0)\zeta^4 + a_6(0)\zeta^5 + \dots, \quad Y(1, \zeta) = \zeta + a_4(1)\zeta^4 + a_5(1)\zeta^5 + \dots, \quad (30, 31)$$

$$Y(2, \zeta) = \zeta^2 + a_3(2)\zeta^4 + a_4(2)\zeta^5 + \dots, \quad Y(3, \zeta) = \zeta^3 + a_2(3)\zeta^4 + a_3(3)\zeta^5 + \dots, \quad (32, 33)$$

$$\Psi(0, \zeta) = 1 + a_3^*(0)\zeta^4 + a_6^*(0)\zeta^5 + \dots, \quad \Psi(1, \zeta) = \zeta + a_4^*(1)\zeta^4 + a_5^*(1)\zeta^5 + \dots, \quad (34, 35)$$

$$\Psi(2, \zeta) = \zeta^2 + a_3^*(2)\zeta^4 + a_4^*(2)\zeta^5 + \dots, \quad \Psi(3, \zeta) = \zeta^3 + a_2^*(3)\zeta^4 + a_3^*(3)\zeta^5 + \dots. \quad (36, 37)$$

It can be shown with the help of equation (6) or (7) that the constants of A_1 - A_4 and B_1 - B_4 used in the solutions for W and Θ , see equations (28) and (29), are related as follows:

$$\begin{bmatrix} 0 & 1 & 0 & 0 \\ 0 & 0 & 2 & 0 \\ 0 & 0 & 0 & 3 \\ 4a_5(0) & 4a_5(1) & 4a_5(2) & 4a_5(3) \end{bmatrix} \begin{bmatrix} A_1/L \\ A_2/L \\ A_3/L \\ A_4/L \end{bmatrix} = -s^2 \begin{bmatrix} \zeta/s^2 & 0 & 2 & 0 \\ 0 & \zeta/s^2 & 0 & 6 \\ 12a_5^*(0) & 12a_5^*(1) & 12a_5^*(2) + \zeta/s^2 & 12a_5^*(3) \\ 20a_6^*(0) & 20a_6^*(1) & 20a_6^*(2) & 20a_6^*(3) + \zeta/s^2 \end{bmatrix} \begin{bmatrix} B_1 \\ B_2 \\ B_3 \\ B_4 \end{bmatrix}. \quad (38)$$

The 4×4 square matrix on the right side was pre-multiplied by the inverse of the 4×4 square matrix of the left side to obtain explicit expressions for the A_1/L , A_2/L , A_3/L and A_4/L . This was achieved by making extensive use of symbolic computation [25, 26] which was essentially desirable because the terms $a_5(0)$, $a_5(1)$, $a_5(2)$, $a_5(3)$, etc., are algebraic expressions and not numbers.

In this way A_1 - A_4 are related to B_1 - B_4 as follows:

$$A_1/L = R_1B_1 + R_2B_2 + R_3B_3 + R_4B_4, \quad A_2/L = R_5B_1 + R_6B_3, \quad (39)$$

$$A_3/L = R_7B_2 + R_8B_4, \quad A_4/L = R_9B_1 + R_{10}B_2 + R_{11}B_3 + R_{12}B_4, \quad (40)$$

where

$$R_1 = C_9/\mu^2, \quad R_2 = (-s^2\mu^2\zeta + C_6\zeta - 3s^2C_{10})/(\mu^2\zeta), \quad R_3 = 2(-3s^2C_7 + s^2C_9 + 3C_2\zeta)/(\mu^2\zeta), \quad (41)$$

$$R_4 = 6C_1/\mu^2, \quad R_5 = -\zeta, \quad R_6 = -2s^2, \quad R_7 = -\zeta/2, \quad R_8 = -3s^2, \quad R_9 = s^2(\mu^2\zeta + C_{10})/(6C_1), \quad (42, 43)$$

$$R_{10} = s^2C_7/3C_1, \quad R_{11} = (-4s^2C_3 + s^2C_6 - C_1\zeta)/(3C_1), \quad R_{12} = 2s^2C_2/C_1. \quad (44)$$

Using the sign convention of Figure 2 and noting that a prime now denotes differentiation with respect to ζ , the expressions for bending moment $M(\zeta)$ and shear force $Q(\zeta)$ can be written as (see Appendix A)

$$M(\zeta) = -(EI/L)(d\Theta/d\zeta) = -(EI/L) [\Psi'(0, \zeta)B_1 + \Psi'(1, \zeta)B_2 + \Psi'(2, \zeta)B_3 + \Psi'(3, \zeta)B_4] \\ = -(EI/L^2) [\Psi'(0, \zeta)B_1L + \Psi'(1, \zeta)B_2L + \Psi'(2, \zeta)B_3L + \Psi'(3, \zeta)B_4L] \quad (45)$$

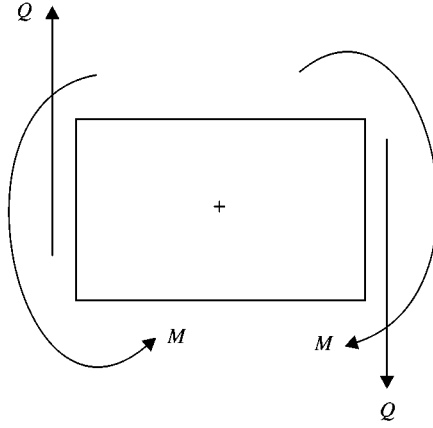


Figure 2. Sign convention for positive shear force (Q) and bending moment (M).

and

$$\begin{aligned}
 Q(\xi) &= -(1/L)dM/d\xi + \rho I\Theta(\omega^2 + \Omega^2) - (T/L)dW/d\xi \\
 &= (EI/L^2)[\Phi_1(\xi)B_1 + \Phi_2(\xi)B_2 + \Phi_3(\xi)B_3 + \Phi_4(\xi)B_4] \\
 &= (EI/L^3)[\Phi_1(\xi)B_1L + \Phi_2(\xi)B_2L + \Phi_3(\xi)B_3L + \Phi_4(\xi)B_4L], \quad (46)
 \end{aligned}$$

where

$$\Phi_1(\xi) = \Psi''(0, \xi) + \tau\Psi(0, \xi) - R_1g(\xi)Y'(0, \xi) - R_5g(\xi)Y'(1, \xi) - R_9g(\xi)Y'(3, \xi), \quad (47)$$

$$\Phi_2(\xi) = \Psi''(1, \xi) + \tau\Psi(1, \xi) - R_2g(\xi)Y'(0, \xi) - R_7g(\xi)Y'(2, \xi) - R_{10}g(\xi)Y'(3, \xi), \quad (48)$$

$$\Phi_3(\xi) = \Psi''(2, \xi) + \tau\Psi(2, \xi) - R_3g(\xi)Y'(0, \xi) - R_6g(\xi)Y'(1, \xi) - R_{11}g(\xi)Y'(3, \xi), \quad (49)$$

$$\Phi_4(\xi) = \Psi''(3, \xi) + \tau\Psi(3, \xi) - R_4g(\xi)Y'(0, \xi) - R_8g(\xi)Y'(2, \xi) - R_{12}g(\xi)Y'(3, \xi), \quad (50)$$

with

$$\tau = r^2(\mu^2 + \eta^2) \quad (51)$$

and

$$g(\xi) = \frac{1}{2}\eta^2(1 + 2\alpha - 2\alpha\xi - \xi^2) + p^2. \quad (52)$$

In order to develop the dynamic stiffness matrix of the rotating Timoshenko beam element the boundary conditions for displacement and forces are imposed.

The end conditions for displacements and forces of the element (see Figure 3) are, respectively, given below.

Displacements:

$$\text{at } \xi = 0: W = \delta_1, \text{ and } \Theta = \Theta_1; \quad \text{at } \xi = 1: W = \delta_2, \text{ and } \Theta = \Theta_2. \quad (53, 54)$$

Forces:

$$\text{at } \xi = 0: Q = Q_1, \text{ and } M = M_1; \quad \text{at } \xi = 1: Q = -Q_2, \text{ and } M = -M_2. \quad (55, 56)$$

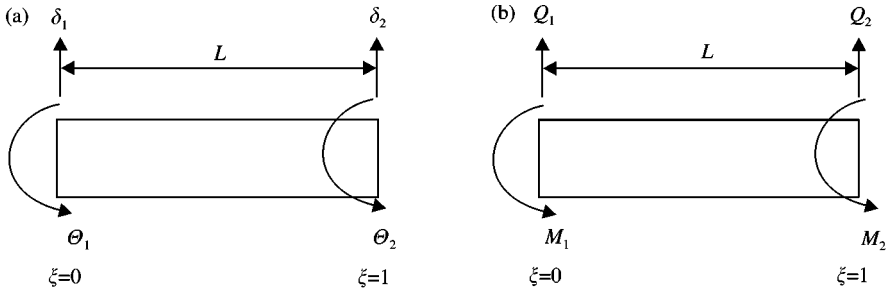


Figure 3. Boundary conditions for (a) displacements and (b) forces of the rotating Timoshenko beam.

Substituting equations (53) and (54) into equations (28) and (29) and equations (55) and (56) into equations (45) and (46) and making use of equations (39, 40) and (47)–(52) give

$$\delta_1 = A_1 = R_1(B_1L) + R_2(B_2L) + R_3(B_3L) + R_4(B_4L), \quad \Theta_1 = B_1, \quad (57, 58)$$

$$\delta_2 = S_1(B_1L) + S_2(B_2L) + S_3(B_3L) + S_4(B_4L), \quad (59)$$

$$\Theta_2 = B_1\Psi(0, 1) + B_2\Psi(1, 1) + B_3\Psi(2, 1) + B_4\Psi(3, 1) \quad (60)$$

and

$$Q_1 = W_3 [\Phi_1(0)B_1L + \Phi_2(0)B_2L + \Phi_3(0)B_3L + \Phi_4(0)B_4L], \quad M_1 = -W_2(B_2L), \quad (61, 62)$$

$$Q_2 = -W_3 [\Phi_1(1)B_1L + \Phi_2(1)B_2L + \Phi_3(1)B_3L + \Phi_4(1)B_4L], \quad (63)$$

$$M_2 = W_2 [\Psi'(0, 1)B_1L + \Psi'(1, 1)B_2L + \Psi'(2, 1)B_3L + \Psi'(3, 1)B_4L], \quad (64)$$

where

$$S_1 = R_1Y(0, 1) + R_5Y(1, 1) + R_9Y(3, 1), \quad S_2 = R_2Y(0, 1) + R_7Y(2, 1) + R_{10}Y(3, 1), \quad (65, 66)$$

$$S_3 = R_3Y(0, 1) + R_6Y(1, 1) + R_{11}Y(3, 1), \quad S_4 = R_4Y(0, 1) + R_8Y(2, 1) + R_{12}Y(3, 1), \quad (67, 68)$$

and

$$W_1 = EI/L, \quad W_2 = EI/L^2, \quad W_3 = EI/L^3 \quad (69)$$

Equations (57)–(60) and (61)–(64) can be written in the following matrix form:

$$\begin{bmatrix} \delta_1 \\ \Theta_1 \\ \delta_2 \\ \Theta_2 \end{bmatrix} = \begin{bmatrix} R_1L & R_2L & R_3L & R_4L \\ 1 & 0 & 0 & 0 \\ S_1L & S_2L & S_3L & S_4L \\ \Psi(0, 1) & \Psi(1, 1) & \Psi(2, 1) & \Psi(3, 1) \end{bmatrix} \begin{bmatrix} B_1 \\ B_2 \\ B_3 \\ B_4 \end{bmatrix} \quad (70)$$

or

$$\delta = \mathbf{GB} \quad (71)$$

and

$$\begin{bmatrix} Q_1 \\ M_1 \\ Q_2 \\ M_2 \end{bmatrix} = \begin{bmatrix} W_3 \Phi_1(0) & W_3 \Phi_2(0) & W_3 \Phi_3(0) & W_3 \Phi_4(0) \\ 0 & -W_2 & 0 & 0 \\ -W_3 \Phi_1(1) & -W_3 \Phi_2(1) & -W_3 \Phi_3(1) & -W_3 \Phi_4(1) \\ W_2 \Psi'(0, 1) & W_2 \Psi'(1, 1) & W_2 \Psi'(2, 1) & W_2 \Psi'(3, 1) \end{bmatrix} \begin{bmatrix} B_1 \\ B_2 \\ B_3 \\ B_4 \end{bmatrix} \quad (72)$$

or

$$\mathbf{F} = \mathbf{HB}. \quad (73)$$

The dynamic stiffness matrix \mathbf{K} can be obtained by eliminating the constant vector \mathbf{B} from equations (71) and (73) to give the force–displacement relationship as

$$\mathbf{F} = \mathbf{K}\delta \quad (74)$$

or

$$\begin{bmatrix} Q_1 \\ M_1 \\ Q_2 \\ M_2 \end{bmatrix} = \begin{bmatrix} k_{11} & k_{12} & k_{13} & k_{14} \\ & k_{22} & k_{23} & k_{24} \\ & & k_{33} & k_{34} \\ & & & k_{44} \end{bmatrix} \begin{bmatrix} \Delta_1 \\ \Theta_1 \\ \Delta_2 \\ \Theta_2 \end{bmatrix}, \quad (75)$$

symmetric

where

$$\mathbf{K} = \mathbf{HG}^{-1} \quad (76)$$

is the required dynamic stiffness matrix.

Each individual element of the matrix \mathbf{K} is generated algebraically by inverting the \mathbf{G} matrix and premultiplying the resulting matrix by the \mathbf{H} matrix. This procedure was greatly assisted by the symbolic computing package REDUCE [25, 26]. The ten independent terms of the \mathbf{K} matrix are obtained as

$$k_{11} = W_3 \lambda_1 / \Delta, \quad k_{12} = k_{21} = W_2 \lambda_2 / \Delta, \quad k_{13} = k_{31} = W_3 \lambda_3 / \Delta, \quad k_{14} = k_{41} = W_2 \lambda_4 / \Delta, \quad (77-80)$$

$$k_{22} = W_1 \lambda_5 / \Delta, \quad k_{23} = k_{32} = W_2 \lambda_6 / \Delta, \quad k_{24} = k_{42} = W_1 \lambda_7 / \Delta, \quad (81-83)$$

$$k_{33} = W_3 \lambda_8 / \Delta, \quad k_{34} = k_{43} = W_2 \lambda_9 / \Delta, \quad k_{44} = W_1 \lambda_{10} / \Delta, \quad (84-86)$$

where

$$\lambda_1 = [S_2 \Phi_4(0) - S_4 \Phi_2(0)] \Psi(2, 1) - [S_2 \Phi_3(0) - S_3 \Phi_2(0)] \Psi(3, 1) - [S_3 \Phi_4(0) - S_4 \Phi_3(0)] \Psi(1, 1), \quad (87)$$

$$\lambda_2 = -[S_3 \Psi(3, 1) - S_4 \Psi(2, 1)]. \quad (88)$$

$$\lambda_3 = [R_4 \Phi_2(0) - R_2 \Phi_4(0)] \Psi(2, 1) + [R_2 \Phi_3(0) - R_3 \Phi_2(0)] \Psi(3, 1) + [R_3 \Phi_4(0) - R_4 \Phi_3(0)] \Psi(1, 1), \quad (89)$$

$$\lambda_4 = [R_2 S_3 - R_3 S_2] \Phi_4(0) + [R_4 S_2 - R_2 S_4] \Phi_3(0) + [R_3 S_4 - R_4 S_3] \Phi_2(0), \quad (90)$$

$$\lambda_5 = [R_1 S_3 - R_3 S_1] \Psi(3, 1) + [R_3 S_4 - R_4 S_3] \Psi(0, 1) + [R_4 S_1 - R_1 S_4] \Psi(2, 1), \quad (91)$$

$$\lambda_6 = [R_3\Psi(3, 1) - R_4\Psi(2, 1)], \quad \lambda_7 = -[R_3S_4 - R_4S_3], \quad (92, 93)$$

$$\lambda_8 = [R_2\Phi_4(1) - R_4\Phi_2(1)]\Psi(2, 1) + [R_4\Phi_3(1) - R_3\Phi_4(1)]\Psi(1, 1) + [R_3\Phi_2(1) - R_2\Phi_3(1)]\Psi(3, 1), \quad (94)$$

$$\begin{aligned} \lambda_9 = & -R_2[\Psi(2, 1)\Psi'(3, 1) - \Psi(3, 1)\Psi'(2, 1)] - R_3[\Psi(3, 1)\Psi'(1, 1) - \Psi(1, 1)\Psi'(3, 1)] \\ & - R_4[\Psi(1, 1)\Psi'(2, 1) - \Psi(2, 1)\Psi'(1, 1)], \end{aligned} \quad (95)$$

$$\lambda_{10} = [R_2S_3 - R_3S_2]\Psi'(3, 1) + [R_4S_2 - R_2S_4]\Psi'(2, 1) + [R_3S_4 - R_4S_3]\Psi'(1, 1), \quad (96)$$

and

$$\Delta = [R_3S_4 - R_4S_3]\Psi(1, 1) + [R_4S_2 - R_2S_4]\Psi(2, 1) + [R_2S_3 - R_3S_2]\Psi(3, 1). \quad (97)$$

The above dynamic stiffness matrix relates to the out-of-plane motion of the beam, in the YZ -plane of Figure 1. The dynamic stiffness matrix for the in-plane motion (in XZ -plane) can be derived in a similar manner by suitable choice of parameters [4, 7].

2.1. APPLICATION OF THE DYNAMIC STIFFNESS MATRIX

The resultant dynamic stiffness matrix can now be used to compute the natural frequencies and mode shapes of a rotating Timoshenko beam with various end conditions. A rotating non-uniform Timoshenko beam, for example a tapered Timoshenko beam, can also be analyzed for its free vibration characteristics by idealizing it as an assemblage of many uniform beams, and is thus treated as a stepped beam (see Figure 1). An accurate and reliable method of calculating the natural frequencies and mode shapes is to use the dynamic stiffness matrix method coupled with the well-known algorithm of Wittrick and Williams [23], which has featured in numerous papers. The algorithm, unlike its proof, is very simple to use [8–10], but for a detailed insight interested readers are referred to the original work of Wittrick and Williams [23]. Basically, the algorithm needs the dynamic stiffness matrices of individual members in a structure and information about their natural frequencies when both ends are clamped. This information is needed to ensure that no natural frequencies of the structure are missed. Thus an explicit expression from which the clamped–clamped natural frequencies can be found facilitates a straightforward application of the algorithm. Δ in equation (97) is such an expression because the clamped–clamped natural frequencies are given by its zeros. It should be noted that the actual requirement of the algorithm is to isolate these clamped–clamped natural frequencies (that is to determine how many such natural frequencies are there below a specified trial frequency) rather than actually calculating them. The Wittrick–Williams algorithm [8–10] essentially gives the number of natural frequencies of a structure that exists below an arbitrarily chosen trial frequency rather than actually calculating the natural frequencies. This simple feature of the algorithm can be used to calculate any natural frequency of the structure to any desirable accuracy.

3. RESULTS AND DISCUSSION

Using the above theory, the natural frequencies of rotating Timoshenko beams with cantilever end conditions were obtained for a range of illustrative examples. The results are

presented in non-dimensional form and can be reproduced by using any set of appropriate data. However, it is instructive to use representative values for k , E/G , r and s (see equations (19)) so that any possibility of numerical ill conditioning (as a result of using unrealistic values) can be avoided. During the current investigation typical numerical values used for k , E/G , r and s are $2/3$, $8/3$, 0.04 and 0.08 respectively. (Note that it can be shown with the help of equation (19) that for $k = 2/3$ and $E/G = 8/3$, $s = 2r$.) It was found that the convergence of the series solution was excellent. From a computational point of view, a total of 120 terms was found to be completely adequate in obtaining results with sufficient accuracy.

References [14, 15], which give natural frequencies of rotating Timoshenko beams with cantilever end condition, were used and a direct comparison of results was made. The authors of reference [14] gave results using the transfer matrix method, but these were reported only for the fundamental natural frequency of the beam. Nevertheless, these results (see their Tables 3 and 4) are reconstructed using the present theory. Tables 1 and 2 show results using the present theory and those reported in reference [14] using the transfer matrix method. (Note that the symbol S used in reference [14] is equal to $1/r$ for the present paper.)

The results of Table 1 illustrate the effect of the rotational speed parameter (η) on the fundamental natural frequency of the Timoshenko beam, and as expected, when $\eta = 0$ complete agreement between the two sets of results is evident. However, the disagreement between the two sets of results increases with increasing rotational speed, and the reason for this is, of course, the fact that the authors of reference [14] omitted the term $\rho I \Omega^2 \theta$ in their formulation (see equation (2)). The effect of the Timoshenko beam parameter r ($= 1/S$) on the fundamental natural frequency of the beam is shown in Table 2 when the rotational speed parameter η is set to 0 and 5 respectively. Here again the results from the present theory match exactly with those of reference [14] for the case when $\eta = 0$ (except ± 1 in the last digit for a few cases, which the author believes is a rounding error in reference [14]). Clearly, the results do not match for the case when $\eta = 5$ because of the above reason. With increasing S (and hence decreasing r) the difference in results diminishes, as expected.

Next, the illustrative examples of reference [15] are used for comparison. Unfortunately, the authors of reference [15] have given only one set of tabulated (*numerical*) results (see their Table 7) and they are only for the fundamental natural frequency of the rotating Timoshenko beam. In contrast, they have given a set of six tabulated (*numerical*) results for the first three natural frequencies of the corresponding Bernoulli–Euler beam

TABLE 1

Fundamental natural frequency of a rotating Timoshenko beam with cantilever end condition for various values of the rotational speed parameter η , with $r_H = 0$, $S^\dagger = 30$ ($r = 1/30$) and $E/kG = 3.059$

η	Fundamental natural frequency (μ_1)		
	Present theory	Reference [14]	Error (%)
0	3.4798	3.4798	0
1	3.6445	3.6452	0.019
2	4.0971	4.0994	0.056
3	4.7516	4.7558	0.088
4	5.5314	5.5375	0.110
5	6.3858	6.3934	0.119

[†] The variable S (instead of r) where $S = 1/r$ is used here for a direct comparison of results with reference [14].

TABLE 2

Fundamental natural frequency of a rotating Timoshenko beam with cantilever end condition for various values of S ($S = 1/r$), when $\eta = 0$ and $\eta = 5$ with $r_H = 0$ and $E/kG = 3.059$

S	$(\eta = 0)$		$(\eta = 5)$	
	Present theory μ_1	Reference [14] μ_1	Present theory μ_1	Reference [14] μ_1
20	3.4364	3.4364	6.3126	6.3241
30	3.4798	3.4798	6.3858	6.3934
40	3.4955	3.4954	6.4131	6.4179
50	3.5028	3.5028	6.4260	6.4294
80	3.5108	3.5108	6.4403	6.4418
100	3.5127	3.5126	6.4436	6.4446
150	3.5145	3.5144	6.4469	6.4476
200	3.5152	3.5152	6.4481	6.4485
300	3.5156	3.5155	6.4489	6.4493

TABLE 3

Fundamental natural frequency of a rotating Timoshenko beam with cantilever end condition for various values of r and η , with $r_H = 0$, $k = 2/3$, $E/G = 8/3$. (The results shown in parentheses are from reference [15].)

r	Fundamental natural frequency (μ_1)			
	$\eta = 0$	$\eta = 4$	$\eta = 8$	$\eta = 12$
0	3.5160 (3.516)	5.5850 (5.585)	9.2568 (9.257)	13.170 (13.170)
0.01	3.5119 (3.512)	5.5791 (5.580)	9.2447 (9.246)	13.148 (13.150)
0.02	3.4998 (3.500)	5.5616 (5.564)	9.2096 (9.215)	13.087 (13.095)
0.03	3.4799 (3.480)	5.5332 (5.539)	9.1549 (9.167)	12.998 (13.015)
0.04	3.4527 (3.453)	5.4951 (5.505)	9.0854 (9.106)	12.893 (12.923)
0.05	3.4187 (3.419)	5.4487 (5.463)	9.0060 (9.036)	12.783 (12.827)
0.06	3.3787 (3.379)	5.3954 (5.415)	8.9208 (8.963)	12.672 (12.734)
0.07	3.3335 (3.333)	5.3370 (5.363)	8.8333 (8.889)	12.564 (12.646)
0.08	3.2837 (3.248) [†]	5.2749 (5.307)	8.7456 (8.815)	12.458 (12.564)
0.09	3.2302 (3.230)	5.2104 (5.249)	8.6588 (8.744)	12.353 (12.487)
0.1	3.1738 (3.174)	5.1448 (5.191)	8.5735 (8.677)	12.247 (12.415)

[†] This figure is taken from reference [15] and is probably in error. It could be a typographical error and the intended value is probably 3.284 instead of 3.248.

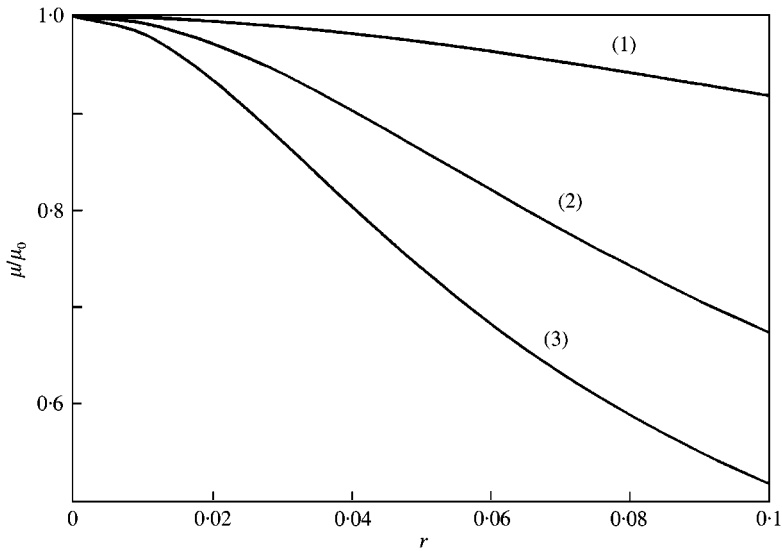


Figure 4. The first three natural frequencies of a rotating Timoshenko beam for the case when $\eta = 4$ (μ_0 corresponds to the natural frequencies of Bernoulli–Euler beam).

(see Tables 1–6, pp. 511–516 of reference [15]) which are actually peripheral to the main investigation. Nevertheless, the results obtained from the present theory are compared with those limited results given in reference [15]. These are shown in Table 3 along with the results of reference [15] shown in parentheses. A complete agreement was expected because the present theory as well as the theory presented in reference [15] are both based on the solution of the governing differential equations, and therefore, both theories are expected to give exact results. This was not to be the case except when $\eta = 0$. As can be seen from the results of Table 3, the discrepancy between the two sets of results increases with increasing values of the rotational speed (η). The reason for this, is again because of the omission of the term $\rho I \Omega^2 \theta$ in equation (2), by the authors of reference [15] (see their equation (10)).

The authors of reference [15] have given some graphical results, showing the variation of the first three natural frequencies of the cantilever Timoshenko beam with the parameter r , for three different values of the rotational speed parameter η (see Figures 5–7 of their paper). Using the present theory, one set of these results, which corresponds to the case $\eta = 4$, is shown in Figure 4 for comparison. A resemblance between this figure and Figure 5 of reference [15] seems apparent. However, when examined and inspected closely by computed results, the discrepancy between the two figures becomes noticeable. Figure 5 shows the difference in the fundamental natural frequency of the rotating Timoshenko beam when using reference [15] and the present theory.

For completeness, two additional sets of results were obtained. Figure 6 shows the first set in which the effect of rotational speed (η) on the first three natural frequencies of the cantilever Timoshenko beam is demonstrated when $r = 0.04$. The natural frequencies, which are non-dimensionalized with respect to the non-rotating case, increase with increasing η because of the centrifugal stiffening effect. As expected, the effect is relatively more pronounced for lower order frequencies than the higher order ones. The final set of results was obtained to assess the errors incurred, as a result of using the Bernoulli–Euler theory, as opposed to Timoshenko theory for the rotating beam. To this end the variation of the percentage error in the third natural frequency with rotational speed (η) is shown in Figure 7 for three different values of r . The error diminishes with rotational speed. This is expected because at higher rotational speed the centrifugal stiffness term dominates the

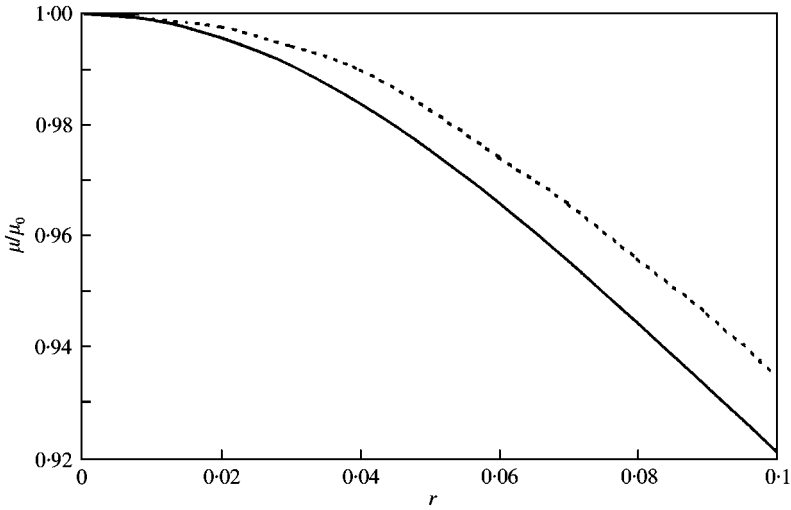


Figure 5. The fundamental natural frequency of a rotating Timoshenko beam using present theory (—) and reference [15] (- - -) for the case when $\eta = 4$ (μ_0 corresponds to the natural frequencies of Bernoulli-Euler beam).

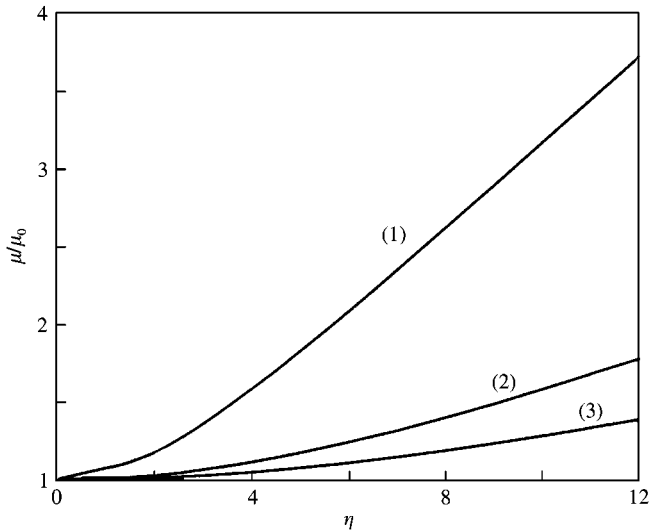


Figure 6. The effect of rotational speed on the first three natural frequencies of a rotating Timoshenko beam (μ_0 corresponds to the natural frequencies of non-rotating Timoshenko beam).

mechanical stiffness term with the latter being influenced by shear deformation and rotatory inertia effects whereas the former is not. The error increases with increasing r as expected.

The free vibration analysis of rotating non-uniform (tapered) Timoshenko beams is outside the scope of this paper. However, such an investigation can be carried out in a similar manner to that described for rotating non-uniform (tapered) Bernoulli-Euler beams in reference [7]. When dealing with the problem the beam is essentially idealized into a number of uniform elements so that it can be treated as a stepped beam which represents the non-uniform (tapered) beam. Naturally, results obtained from such a model will not be exact, but will be sufficiently accurate depending on the number of elements used. Due to the use of dynamic stiffness elements, such as idealization will no-doubt, have better model

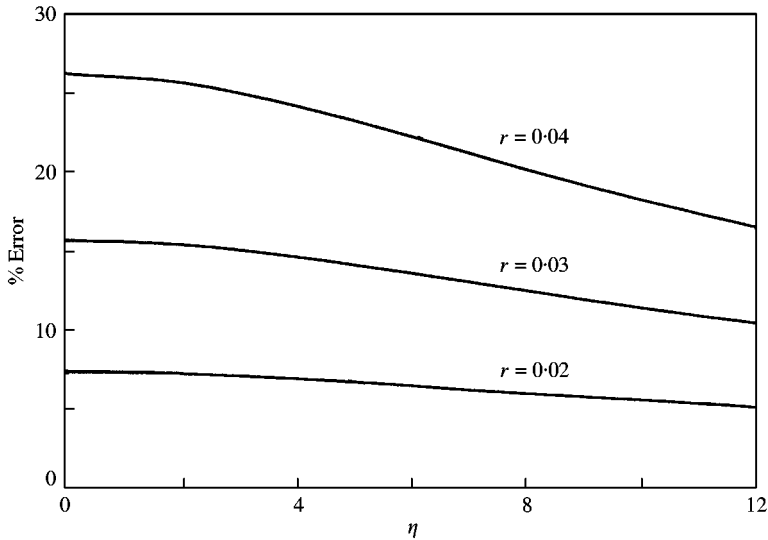


Figure 7. Percentage error in the third natural frequency of a rotating beam when using Bernoulli–Euler beam theory as opposed to Timoshenko theory.

accuracy [7] than the traditional finite element method. A detailed procedure for improving the accuracy from approximate results by using a parabolic limit is described in reference [7]. The same procedure (which basically minimizes the discretization error) can be used for rotating non-uniform (tapered) Timoshenko beams.

4. CONCLUSIONS

Starting from the governing differential equations of motion in free vibration, an exact dynamic stiffness theory has been developed for a rotating Timoshenko beam. The theory is applied in conjunction with the Wittrick–Williams algorithms to compute the natural frequencies of rotating Timoshenko beams with cantilever end condition. The results obtained from the present theory are compared with published results and the predictable accuracy of the dynamic stiffness theory is confirmed. The effects of rotatory inertia, shear deformation and rotational speed on the natural frequencies of rotating Timoshenko beams are demonstrated by numerical results. During the course of this investigation an error in the published literature, which devalue the theory, was detected, and was judiciously corrected.

ACKNOWLEDGMENTS

The author is grateful to his colleague Adam Sobey who first called his attention to the error in the published literature, which partly motivated this research.

REFERENCES

1. D. H. HODGES and M. J. RUTKOWSKI 1981 *American Institute of Aeronautics and Astronautics Journal* **19**, 1459–1466. Free vibration analysis of rotating beams by a variable order finite element method.
2. A. WRIGHT, C. SMITH, R. THRESHER and J. WANG 1982 *Journal of Applied Mechanics* **49**, 197–202. Vibration modes of centrifugally stiffened beams.

3. K. M. UDUPA and T. K. VARADAN 1990 *Journal of Sound and Vibration* **138**, 447–456. Hierarchical finite element method for rotating beams.
4. S. NAGULESWARAN 1994 *Journal of Sound and Vibration* **176**, 613–624. Lateral vibration of a centrifugally tensioned uniform Euler–Bernoulli beam.
5. S. NAGULESWARAN 1997 *Journal of Sound and Vibration* **200**, 63–81. Out of plane vibration of a uniform Euler–Bernoulli beam attached to the inside of a rotating rim.
6. H. H. YOO and S. H. SHIN 1998 *Journal of Sound and Vibration* **212**, 807–828. Vibration analysis of rotating cantilever beams.
7. J. R. BANERJEE 1999 *Journal of Sound and Vibration* **233**, 857–875. Free vibration of centrifugally stiffened uniform and tapered beams using the dynamic stiffness method.
8. F. W. WILLIAMS and W. H. WITTRICK 1983 *Journal of Structural Engineering, American Society of Civil Engineers* **109**, 169–187. Exact buckling and frequency calculations surveyed.
9. F. W. WILLIAMS 1993 *Computers and Structures* **48**, 547–552. Reviews of exact buckling and frequency calculations with optional multi-level substructuring.
10. J. R. BANERJEE 1997 *Computers and Structures* **63**, 101–103. Dynamic stiffness formulation for structural elements: a general approach.
11. R. O. STAFFORD and V. GIURGIUTIU 1975 *International Journal of Mechanical Sciences* **17**, 719–727. Semi-analytic methods for rotating Timoshenko beams.
12. V. GIURGIUTIU and R. O. STAFFORD 1977 *Vertica* **1**, 291–306. Semi-analytic methods for frequencies and mode shapes of rotor blades.
13. T. YOKOYAMA 1988 *International Journal of Mechanical Sciences* **30**, 743–755. Free vibration characteristics of rotating Timoshenko beams.
14. S. Y. LEE and Y. H. KUO 1993 *Journal of Sound and Vibration* **162**, 243–250. Bending frequency of a rotating Timoshenko beam with general elastically restrained root.
15. H. DU, M. K. LIM and K. M. LIEW 1994 *Journal of Sound and Vibration* **175**, 505–523. A power series solution for vibration of a rotating Timoshenko Beam.
16. A. BAZOUNE, Y. A. KHULIEF and N. C. STEPHEN 1999 *Journal of Sound and Vibration* **219**, 157–154. Further results for modal characteristics of rotating tapered Timoshenko beams.
17. G. M. L. GLADWELL and D. K. VIJAY 1975 *Journal of Sound and Vibration* **42**, 387–397. Natural frequencies of free finite-length circular cylinders.
18. J. R. HUTCHINSON 1980 *Transaction of American Society of Mechanical Engineers Journal of Applied Mechanics* **47**, 901–907. Vibration of solid cylinders.
19. K. M. LIEW, K. C. HUNG and M. K. LIM 1995 *Transaction of American Society of Mechanical Engineer Journal of Applied Mechanics* **62**, 159–165. Free vibration studies on stress free three-dimensional elastic solids.
20. K. M. LIEW and K. C. HUNG 1995 *International Journal of Solids and Structures* **32**, 3499–3513. Three-dimensional vibratory characteristics of solid cylinders and some remarks on simplified beam theories.
21. K. C. HUNG, K. M. LIEW and M. K. LIM 1995 *Acta Mechanica* **113**, 37–52. Free vibration of cantilevered cylinders-effects of cross-sections and cavities.
22. K. M. LIEW, K. C. HUNG and M. K. LIM 1997 *Journal of Sound and Vibration* **200**, 505–518. Three-dimensional vibration analysis of solid cylinders of polygonal cross-section using the p-Ritz method.
23. W. H. WITTRICK and F. W. WILLIAMS 1971 *Quarterly Journal of Mechanics and Applied Mathematics* **24**, 263–284. A general algorithm for computing natural frequencies of elastic structures.
24. W. P. HOWSON and F. W. WILLIAMS 1973 *Journal of Sound and Vibration* **26**, 503–515. Natural frequencies of frames with axially loaded Timoshenko members.
25. J. FITCH 1985 *Journal of Symbolic Computing* **1**, 211–227. Solving algebraic problems with REDUCE.
26. G. RAYNA 1986 *REDUCE Software for Algebraic Computation*. New York: Springer-Verlag.

APPENDIX A: DERIVATION OF THE GOVERNING DIFFERENTIAL EQUATIONS OF MOTION OF A ROTATING TIMOSHENKO BEAM

Using the co-ordinate system and notation of Figure 1(b), the uniform strain $\varepsilon_0(y)$ of the cross-section at a distance y from the origin of the rotating Timoshenko beam due to the

action of the centrifugal force $T(y)$ alone is given by

$$\varepsilon_0(y) = T(y)/EA. \quad (A1)$$

where E is Young's modulus and A is the area of cross-section and

$$T(y) = \int_y^L \rho A \Omega^2 (r_i + y) dy = \rho A \Omega^2 \{r_i(L - y) + (L^2 - y^2)/2\}. \quad (A2)$$

Note that the outboard force F at the right-hand end of the beam, see Figure 1(b) and equation (3), is omitted here for simplicity and is unnecessary in the derivation of the governing differential equations.

The axial displacement $u_0(y)$, which is uniform across the cross-section, is related to the strain $\varepsilon_0(y)$ by

$$u'_0(y) = \varepsilon_0(y) = T(y)/EA. \quad (A3)$$

where the prime denotes differentiation with respect to y .

By introducing a flexural displacement $w(y)$ of the beam neutral axis in the Z -direction for an element of length dy at a distance y from the origin and following Timoshenko's beam theory, under flexural displacement (w) and section rotation (θ) the shearing strain (γ) induced in the element is given by

$$\gamma = w' - \theta. \quad (A4)$$

As a result of the combined axial and flexural displacements, the element dy will undergo the following deformations. On the left-hand face of the element, a point at a distance $\bar{\eta}$ away from the neutral axis in the Z direction will have the co-ordinates $\{0, (y + u_0 - \bar{\eta}\theta), (\bar{\eta} + w)\}$ whereas the corresponding point on the right-hand face will have the co-ordinates $[0, \{y + u_0 - \bar{\eta}\theta + (1 + u'_0 - \bar{\eta}\theta') dy\}, (\bar{\eta} + w + w' dy)]$.

Thus, the strain of the element at a distance $\bar{\eta}$ from the neutral axis is given by

$$\varepsilon(y, \eta) = [(1 + u'_0 - \bar{\eta}\theta')^2 + (w')^2] - 1 \cong u'_0 - \bar{\eta}\theta' + \frac{1}{2}(w')^2. \quad (A5)$$

The strain energy due to flexure U_f then follows as

$$U_f = \iiint_V \frac{E\varepsilon^2}{2} dV = \frac{E}{2} \int_A \int_0^L \{(u'_0 - \bar{\eta}\theta' + \frac{1}{2}(w')^2)\}^2 dy dA. \quad (A6)$$

Since the neutral axis passes through the centroid and the area (A) and the second moment of area (I) of the cross-section are, respectively, given by $A = \int_A dA$ and $I = \int_A \bar{\eta}^2 dA$, U_f can be simplified as

$$U_f = \frac{EA}{2} \int_0^L (u'_0)^2 dy + \frac{EI}{2} \int_0^L (\theta')^2 dy + EA \int_0^L u'_0(w')^2 dy. \quad (A7)$$

Using equations (A2) and (A3) and expressing u'_0 in terms of the centrifugal tension $T(y)$

$$U_f = C_1 + \frac{1}{2} \left[\int_0^L EI(\theta')^2 dy + \int_0^L T(w')^2 dy \right]. \quad (A8)$$

where C_1 is a constant and T is given by equation (A3).

The strain energy due to shear U_s is given by

$$U_s = \iiint_V \frac{G\gamma^2}{2} dV = \frac{1}{2} \int_A \int_0^L G\gamma^2 dA dy = \frac{1}{2} kAG \int_0^L \gamma^2 dy. \quad (A9)$$

where G is the shear modulus, k is the section shape factor so that kAG is the shear rigidity of the beam cross-section.

Substituting the expression for γ from equation (A4) into equation (A9) gives

$$U_s = \frac{1}{2} \int_0^L kAG(w' - \theta)^2 dy. \quad (\text{A10})$$

The total strain energy \mathcal{U} of the beam is given by

$$\mathcal{U} = U_f + U_s = \frac{1}{2} \left[\int_0^L \{EI(\theta')^2 + T(w')^2 + kAG(w' - \theta)^2\} dy \right] + C_1. \quad (\text{A11})$$

The kinetic energy of the rotating Timoshenko beam element can be expressed in terms of the velocity components of the point at a distance $\bar{\eta}$ from the neutral axis. From Figure 1(b), the three components of the velocities of this point in the X , Y and Z directions are, respectively, given by

$$V_x = -\Omega(y + u_0 - \bar{\eta}\theta), \quad V_y = -\bar{\eta}\dot{\theta}, \quad V_z = \dot{w}. \quad (\text{A12})$$

Thus, the kinetic energy \mathcal{F} of the rotating Timoshenko beam can be expressed as

$$\mathcal{F} = \frac{1}{2} \int_A \int_0^L (V_x^2 + V_y^2 + V_z^2) \rho dA dy. \quad (\text{A13})$$

Substituting equation (A12) into equation (A13) gives

$$\begin{aligned} \mathcal{F} = \frac{1}{2} \left[\int_A \int_0^L \rho \Omega^2 (y + u_0)^2 dy dA + \int_A \int_0^L \rho \Omega^2 \bar{\eta}^2 \theta^2 dy dA - \int_A \int_0^L 2\rho \Omega^2 \bar{\eta} (y + u_0) \theta dy dA \right. \\ \left. + \int_A \int_0^L \rho \bar{\eta}^2 \dot{\theta}^2 dy dA + \int_A \int_0^L \rho \dot{w}^2 dy dA \right]. \end{aligned} \quad (\text{A14})$$

The first of the above integrals is constant and the third one is zero so that the kinetic energy \mathcal{F} takes the following simplified form:

$$\mathcal{F} = C_2 + \frac{1}{2} \left[\int_0^L \rho I (\Omega^2 \theta^2 + \dot{\theta}^2) dy + \int_0^L \rho A \dot{w}^2 dy \right], \quad (\text{A15})$$

where C_2 is a constant.

The Lagrangian $\mathcal{L} = \mathcal{F} - \mathcal{U}$ can now be formulated as

$$\mathcal{L} = \frac{1}{2} \int_0^L [\rho I (\dot{\theta}^2 + \Omega^2 \theta^2) + \rho A \dot{w}^2] - \{EI(\theta')^2 + T(w')^2 + kAG(w' - \theta)^2\} dy + C_2 - C_1. \quad (\text{A16})$$

Hamilton's principle states that $\delta \int_{t_1}^{t_2} \mathcal{L} dt$ taken between arbitrary intervals of time (t_1, t_2) is stationary for a dynamic trajectory. Therefore

$$\delta \int_{t_1}^{t_2} \mathcal{L} dt = 0. \quad (\text{A17})$$

Substituting equation (A16) into equation (A17) gives

$$\begin{aligned} \int_{t_1}^{t_2} \int_0^L [\rho I (\dot{\theta} \delta \dot{\theta} + \Omega^2 \theta \delta \theta) + \rho A \dot{w} \delta \dot{w}] - \{EI\theta' \delta \theta' + (Tw') \delta w' + kAG(w' - \theta)(\delta w' - \delta \theta)\} \\ \times dy dt = 0. \end{aligned} \quad (\text{A18})$$

On integrating by parts there follows

$$\begin{aligned} & \int_{t_1}^{t_2} \int_0^L [\{(Tw')' - \rho A \ddot{w} + kAG(w' - \theta)\} \delta w + \{EI\theta'' + kAG(w' - \theta) - \rho I \ddot{\theta} + \rho I \Omega^2 \theta\} \delta \theta] dt \\ & + \int_{t_1}^{t_2} [-EI\theta' \delta \theta]_0^L dt + \int_{t_1}^{t_2} [-\{Tw' + kAG(w' - \theta)\} \delta w]_0^L dt + \int_0^L [\rho I \dot{\theta} \delta \theta + \rho A \dot{w} \delta w]_{t_1}^{t_2} \\ & \times dy = 0. \end{aligned} \quad (\text{A19})$$

Since δw and $\delta \theta$ are completely arbitrary, the differential equations of motion follow from the above equation as

$$(Tw')' - \rho A \ddot{w} + kAG(w' - \theta) = 0 \quad (\text{A20})$$

and

$$EI\theta'' + kAG(w' - \theta) - \rho I \ddot{\theta} + \rho I \Omega^2 \theta = 0. \quad (\text{A21})$$

From the natural boundary conditions, equation (A19) gives the expression for bending moment (M) and shear force (Q) as

$$M = -EI\theta' \quad (\text{A22})$$

and

$$Q = -Tw' - kAG(w' - \theta) = -Tw' - M' - \rho I \ddot{\theta} + \rho I \Omega^2 \theta. \quad (\text{A23})$$